Discrete Modeling of Dune-Obstacle Interactions and Dynamics

Horacio Moreno Montanes, Jess Yang, ZhengXu Tang

February 12, 2023

1 Introduction
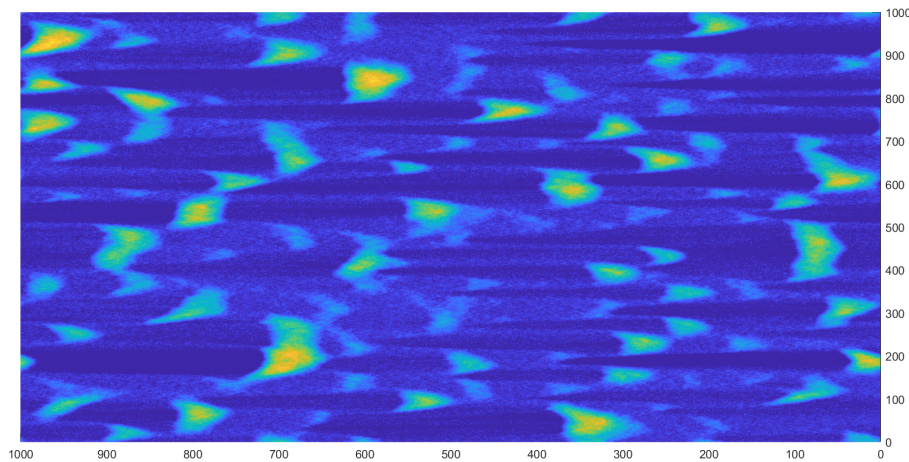

Figure 1: Dune shape at t=500

As desertification worsens, more and more people are starting to be interested in sand control. Predicting and influencing dune movements is the key to achieving this goal. Because dunes are spread over hundreds of kilometers, it has been calculated for decades and centuries. In this case, relying on field observations or satellite observations will become very inefficient. Mathematical modeling is the perfect answer to this kind of problem. Mathematical modeling has been used in many research fields and engineering areas to help analyze. The prediction of the future is the top priority for our discussion. The dune field is a typical nonlinear open system. The input and output of energy information and the nonlinear superposition constitute their essence. There exist several models for dune formation and morphology, which are outlined in [5]. From these models, works by Bishop et al. [3] stand out both in their simplicity and qualitative accuracy to describe the dune formation phenomenon compared to other projects, where people used a series of complex mathematical formulas to design models. In this project, we will worked to improve Bishop's mathematical model to take into account the interaction between dunes and obstacles, an open problem for these discrete models as outlined in the summary of the work in the field [5]. By investigating the collision of dunes and different obstacles ranging in size, we look to replicate physical results observed in dune-obstacle interactions by Bacik et al [2]. In this project, we find that the model can accurately predict some qualitative aspects and quantitative trends such as dune shape and size, but fails to address physical effects such as sand accumulation around the obstacle and changes to dune migration speed as a result of the obstacle collisions.

2 Modeling and Implementation

2.1 Original Model

Our model was adapted from a previous study by Bishop et al.[3]. This model assumes a starting configuration of a perfectly flat, dry desert, where wind only blows from one direction and the velocity of wind is unchanged during the experiment. The dune field is modeled by a square lattice with dimensions L_s and periodic boundaries, where each grid space has an equal side length. The field is covered by evenly distributed sand slabs, each with the same length and width, which enables a slab to fit in one grid space. To allow for greater definition in the vertical direction without sacrificing computation time, the height of the slab is set to be $1/3$ of its width and length. (insert the picture of a sand slab and annotation) As sand slabs can pile up at each grid space, the height of sand at grid position (i, j) can be expressed as the following equation:
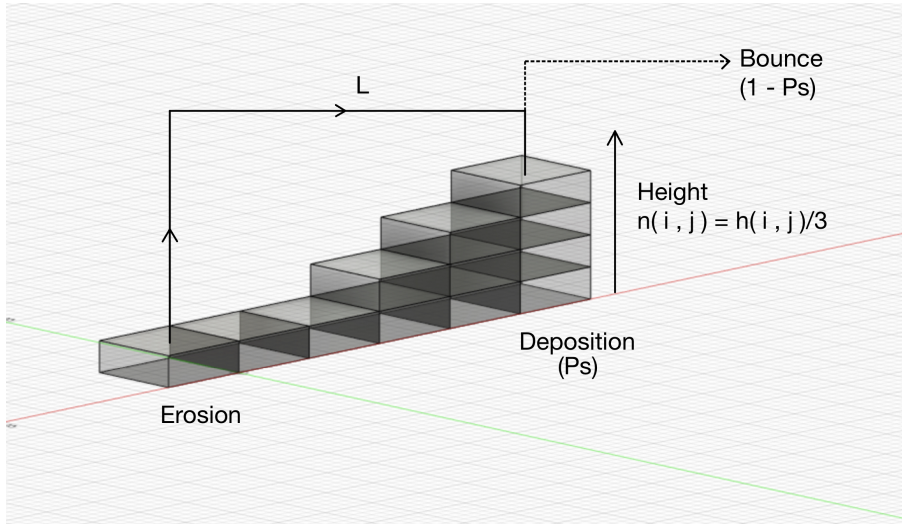

Figure 2: movement of the dune

$$\eta(i, j) = \frac{1}{3}h(i, j), \tag{1}$$

where $\eta(i, j)$ is the height and $h(i, j)$ is the number of sand slabs at (i, j).

When sand slabs pile up and dunes get taller, the windward slabs block wind from affecting the slabs in the lee of the dunes. Therefore, we introduce the concept of shadowzone (See figure c). The shadowzone is the triangular area under the line between a dune crest and the ground with a fixed angle θ_{sz}. When a slab lands on this area, it will stay here. Also, slabs in the area do not move to other sites.

There are 2 ways of sand transportation: by wind and by avalanche. Here we assume the direction of wind is parallel to the horizontal axis in (b).

Dune formation is achieved by repeating the following algorithm: at the beginning of each iteration, a random slab (i, j) is chosen for erosion. The slab travels in the direction of the wind a distance L, which is calculated by the following formula:

$$L(i, j) = \begin{cases} L_0 + C_1(h(i, j) - h_{ref}) + C_2(h(i, j) - h_{ref})^2 & h(i, j) \geq h_{ref} \\ L_0 + C_1(h(i, j) - h_{ref}) & h(i, j) < h_{ref} \end{cases} \tag{2}$$

where

$$h_{ref} = h_{avg} - \frac{1}{2L_s^2} \sum_{(i,j)=(0,0)}^{(L_s-1, L_s-1)} |h(i, j) - h_avg| \tag{3}$$

2

For motivation and explanation for equations (2) and (3), refer to [4] and [3].

The coordinates of the new location for the slab are given by $(i + L(i,j), j)$. Once the slab lands on the new site, there are two possibilities, either the slab will stay at the new site $(i + L(i,j), j)$ with some probability P_d or the slab will bounce to a new site. This deposition probability (the probability of staying at a site) depends on where the slab lands. If the new site $(i + L(i,j), j)$ is a part of a shadowzone, the slab will not bounce to other sites, and the deposition probability is goven by $P_d = 1$. If not, we check if the site has any other sand slabs on it. Here we assume if a site has no sand slabs, the contact surface between the ground and the incoming slab will be harder, and at a higher probability the slab will bounce to other sites. Therefore, if a slab lands on a space in the lattice where there are no other sand slabs, the deposition probability is given by $P_d = P_{ns}$. Otherwise, we have that $P_d = P_s$.

If the sand slab bounces, the process is repeated, and the new distance travelled is calculated by the distance $L(i + L(i,j), j)$. The new site will then be $(i + L(i,j) + L(i + L(i,j), j), j)$. Again, the slab will have a probability of bouncing again or not. Illustrations of sand transport and the shadowzone are illustrated in Figure **??**.It is important to note that for this particular model, one time step is given by Ls^2 iterations of the sand transport process.
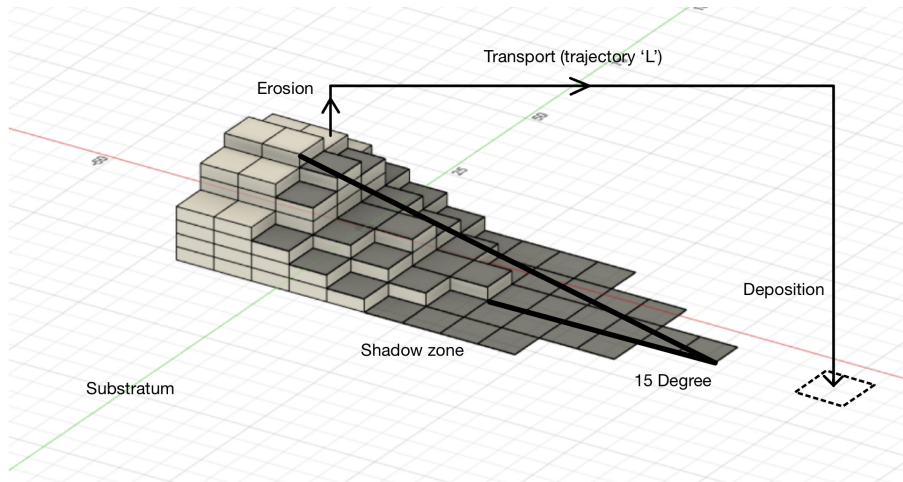

Figure 3: Figure illustrating sand transport and shadowzone

Another way of movement is by avalanche. As a dune gets steeper, the difference in heights of the peak and the surrounding areas gets larger and the top of the dune will fall onto the lower area. In this model, assume the threshold is 3 sand slabs, which is equivalent to the angle of repose of 33.7 degrees for the nearest neighboring sites and 25.2 degrees for the second nearest, respectively [3]. When the difference between the number of slabs at two neighboring sites exceeds 3 slabs, The highest slab will fall to the lower site. Here the neighboring sites of (i,j) are defined as $(i \pm 1, j \pm 1)$. If an avalanche occurs, and a slab moves from (i,j) to some neighboring site (i', j'), then the process for checking if an avalanche occurs at this new location is repeated, and so on until no more avalanches occur. Every time a sand slab is transported, it is checked whether an avalanche occurs both at the position where the sand slab was and where it was deposited.

2.2 Addition of Obstacles to the Model

In order to explore how obstacles affect the behavior of dunes, we introduce cubic obstacles, with side lengths of h_{obs} to the existing model. The size of each obstacle varies from $h_{obs} = 10$ to $h_{obs} = 30$ in increments of 5 to study the size effects of obstacles on dune movement. We assume obstacles cannot be eroded by the air and their shape cannot be changed by any means such as erosion and avalanches. Therefore, obstacles can be effectively seen as "permanent dunes".
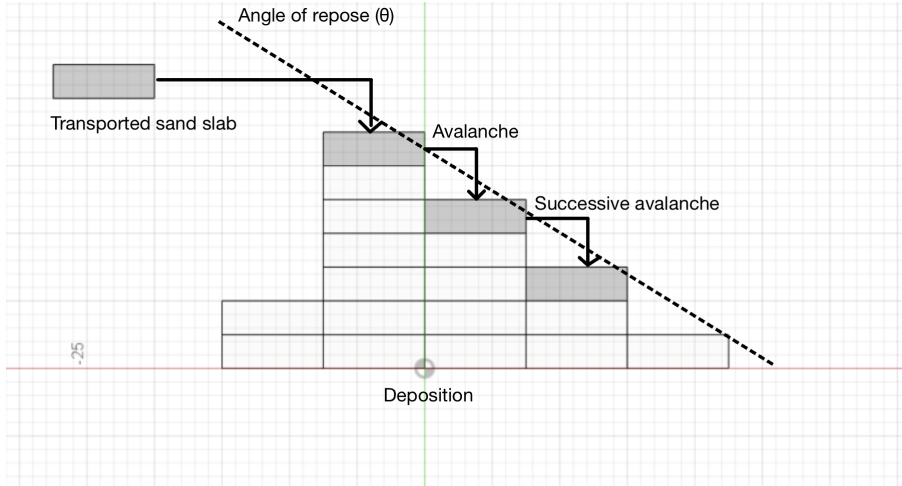
3

Figure 4: movement of the dune

To introduce this obstacle, a lattice of size $L_s = 500$ and starting height of 2 was evolved for 500 time steps to form barchan dunes [1]. A single dune was isolated and the obstacle was placed in its direct path downwind. This can be visualized in Figure 6. After this, the lattice was further evolved for 300 more time steps, enough for two collisions to occur.
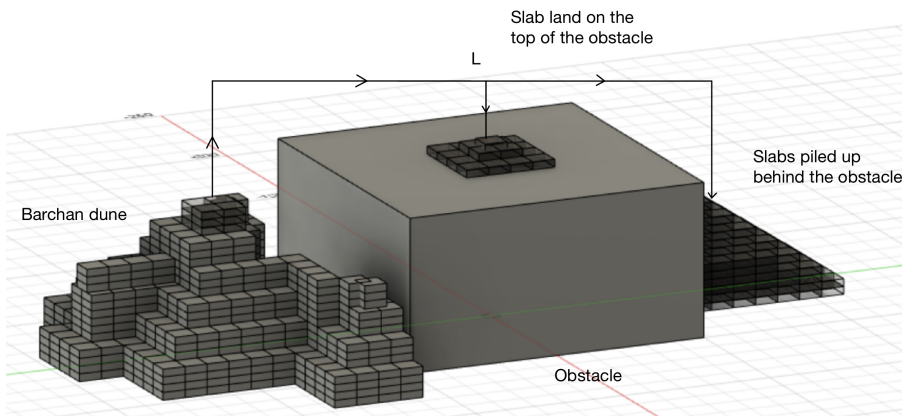

Figure 5: dune-obstacle

3   Results and Analysis

In this project we look at both qualitative and quantitative results to assess and evaluate the model in question. First, we look into the qualitative effects that the obstacle has with respect to the evolution of the dune as it traverses the lattice.

3.1   Qualitative Results and Analysis

Figure 7 shows 3D plots for the process of the collision for four different times, covering the entire event. This figure shows some of the morphological changes that the dune goes through after the collision, which will be expanded on later in this section.

Figure 8 depicts the evolution of the dune at three different stages for different obstacle sizes, as well as one with no obstacle for reference. Wind blows from the top of the figure down, and therefore the dune traverses the lattice in that direction as well. First, it can be noted
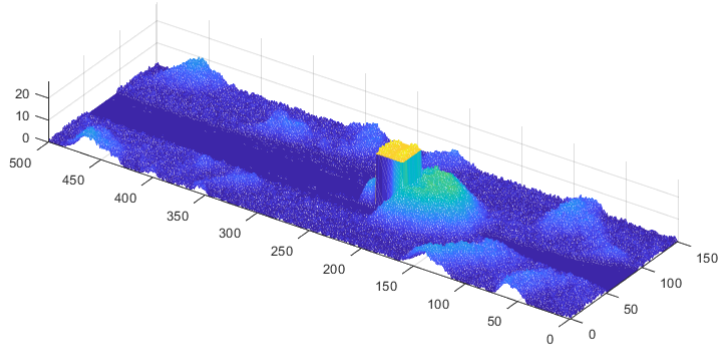
Figure 6: Initial configuration of dune-obstacle interaction for $h_{obs} = 20$.

that we start seeing qualitative changes to the shape of the dune from $h_{obs} = 15$ after one and two collisions, shown in figures 8b and 8c respectively. We can see that there is sand that is deposited from the dune to the area behind the object. The larger the object, the more sand deposited and the greater the deformation caused to the dune shape. For the smallest object with $h_{obs} = 10$, there is virtually no change to the dune shape compared to the dune with a clear path. After $h_{obs} = 15$, there are small spokes formed towards the corners, and these spokes grow larger as more sand from the posterior of the dune is deposited behind the object. Qualitatively, this agrees with the results from physical experiments done by Bacik et al. [2], as larger objects cause a decrease in dune volume. These results can be seen more clearly in 3D in figure 7.

In Figure 8c it can also be noted a decrease in height and asymmetry generated by larger obstacles. At the same time, it is important to note that after 300 time steps, dunes colliding against all obstacles have travelled roughly the same distance. In physical experiments, dunes were observed to travel at slower speeds for larger obstacles [2], which disagrees with our model. This will be further expanded on when looking at the qualitative results of the model.

Finally, we can also see that contrary to expected physical interactions between sand and dunes, there is no sand accumulation in front of the obstacle. This is due to the implementation of the model which does not account for head-on collisions of sand particles against the obstacle. Further improvements of this model should take this into account.

3.2 Quantitative Results and Analysis

Quantitatively, we are interested in two main qualities that were measured in physical experiments: dune transport velocity and dune cross sectional area. Both of these variables were shown to change as dunes collided with different obstacles. Rather than focusing on exact figures, given the nature of the model, we are more interested to investigate whether the trends and relationships between obstacle size and dune velocity and cross sectional area agree.

First, we investigate velocity of the dune as a function of obstacle size. To do so, the dune position was tracked as a function of time. The dune position was calculated by tracking the highest point in the cross section of the dune, obtained by the plane that intersects the obstacle in the center perpendicular to the direction of travel. This method was used contrary to tracking
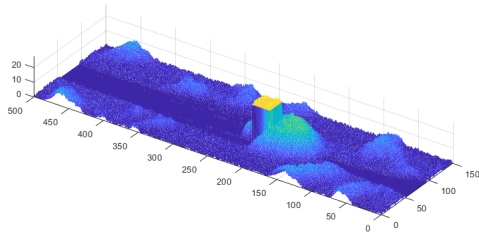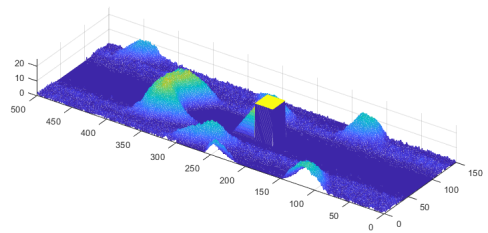
(a) $t = 25$
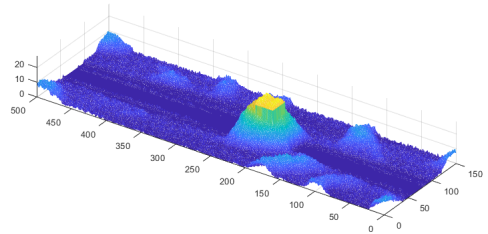
(b) $t = 50$
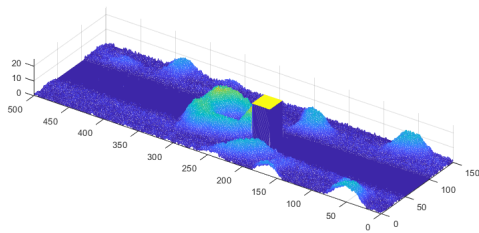
(c) $t = 90$

(d) $t = 125$

Figure 7: Obstacle-dune interaction for $h_{obs} = 20$.

other qualities of the dune such as its center of mass or average horizontal position as these quantities varied greatly during the collision process. The results of this are depicted in figure 9.

We can see that velocities remain relatively constant after each collision for all obstacle sizes. Collisions occur at $t \approx 50$ and $t \approx 250$. Despite the velocity being constant, as dune displacement appears to be linear, there is a slight deviation from the average velocity starting around $t = 100$. However, given that this deviation is also observed in the simulation where there was no obstacle present, therefore we cannot attribute this to the dune-obstacle interaction. For $h_{obs} = 30$, we can also observe some steep changes to the dune position around $t = 100$ and $t = 250$, which can be attributed to the severe deformation that occurs after collision for larger objects. In order to track the velocity of the dune in future simulations where larger objects are present, alternative methods for calculating the distance travelled as a function of time should be explored to take into account these cases.

Average velocity was calculated by performing a linear fit of the data for each obstacle size, and recording the slope of the line of best fit. Results for this can be found in Table 1. As mentioned previously in the qualitative analysis, contrary to results found by Bacik et al., dune velocity remained constant as obstacle height changed. The only exception to this was $h_{obs} = 30$, where there there is a slight increase in the average velocity of the dune. Given the stochastic nature of the model, further simulations with these same parameters would be useful to investigate whether this increase in velocity was a result of the change in height or is unique to the evolution of the dune in this particular simulation. Regardless, this model fails to capture the trend of decreasing velocity observed in physical experiments. This could be the product of several different causes. One of this could be the fact that this decrease in velocity

6

(a) Dune before collision ($t = 0$).

(b) Dune after first collision ($t = 100$).
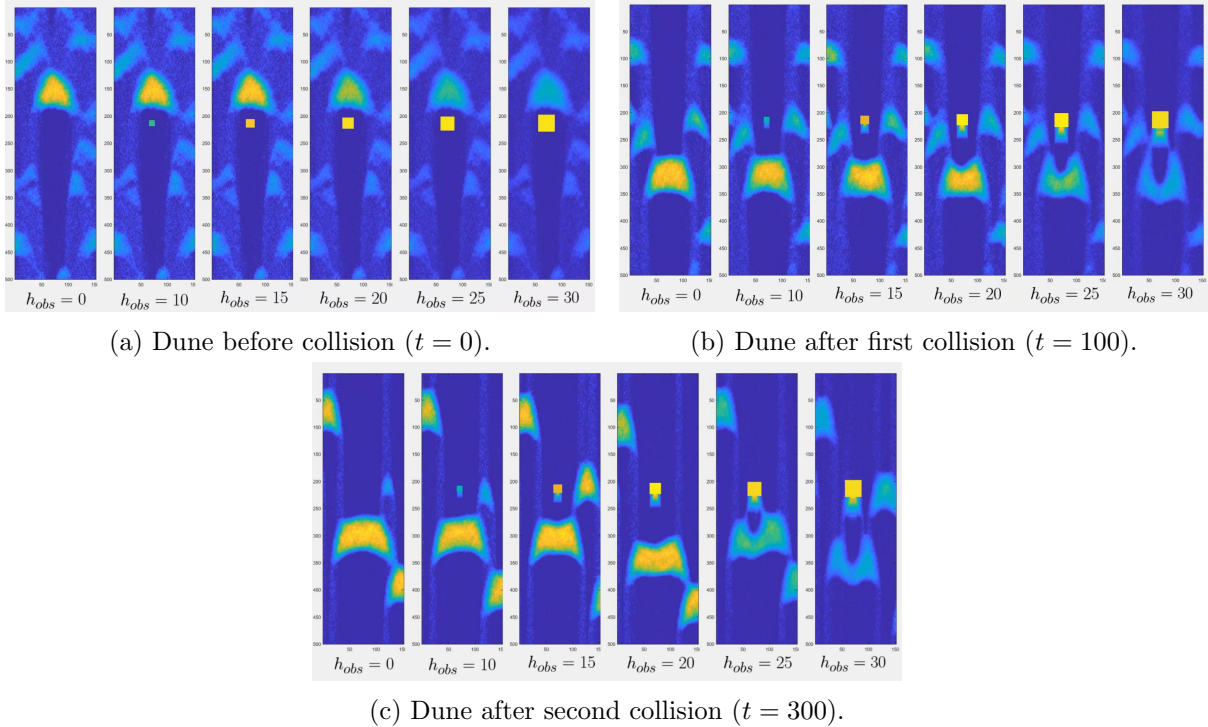

(c) Dune after second collision ($t = 300$).

Figure 8: Dune shape before collision, after first collision, and after second collision with obstacles of different sizes.

is largely due by the change in wind speed and direction caused by the object. Given the way that sand wind transport is modeled in these simulations, assumed to be unidirectional and mostly constant, this particular model is not a good approach to capture this effect. Secondly, turbulence and other effects that contribute to the change in wind flow created by objects like the obstacles introduced are not accounted for at all in the model due to its simple nature.

To add to this, none of the obstacles introduced caused the complete stop to the displacement of the dune, as observed by larger objects [2]. Again, this could be due to the implementation of obstacles for this particular model, where sand particles that travel a long enough distance are allowed to travel through the obstacle rather than colliding with it. Further improvements to the model to take this effect into account could help replicate effects such as this one.

In addition to velocity, dune cross sectional areas were also investigated. Denoted A, this areas can be found in Table 1 before collisions, after the first collision, and after the second collision. It can be seen that for all obstacles, this cross-sectional area which is used as a measure of the size of the dune does decrease, and it decreases more for larger obstacles, agreeing with physical observations. It is important to note, however, that cross sectional area may not be the best metric for dunes colliding with larger objects as these collisions often cause deformation as shown in Figure 8c for $h_{obs} = 30$. Note that compared to other dunes for smaller objects which have a relatively constant depth, collisions with larger objects and loss of sand heavily alter the dune morphology towards the center of the obstacle, thus causing a smaller cross-sectional area that may not accurately reflect the size of the entire dune.

4 Discussion

In this paper, we developed a model based on the simplified dune formation process. For sand dunes, we assume that the sand dunes are in an absolutely dry closed space, which means that they will only be affected by wind and obstacles. The model introduces obstacles under two assumptions: fixed in a position, and their shape remains unchanged. In our study, we
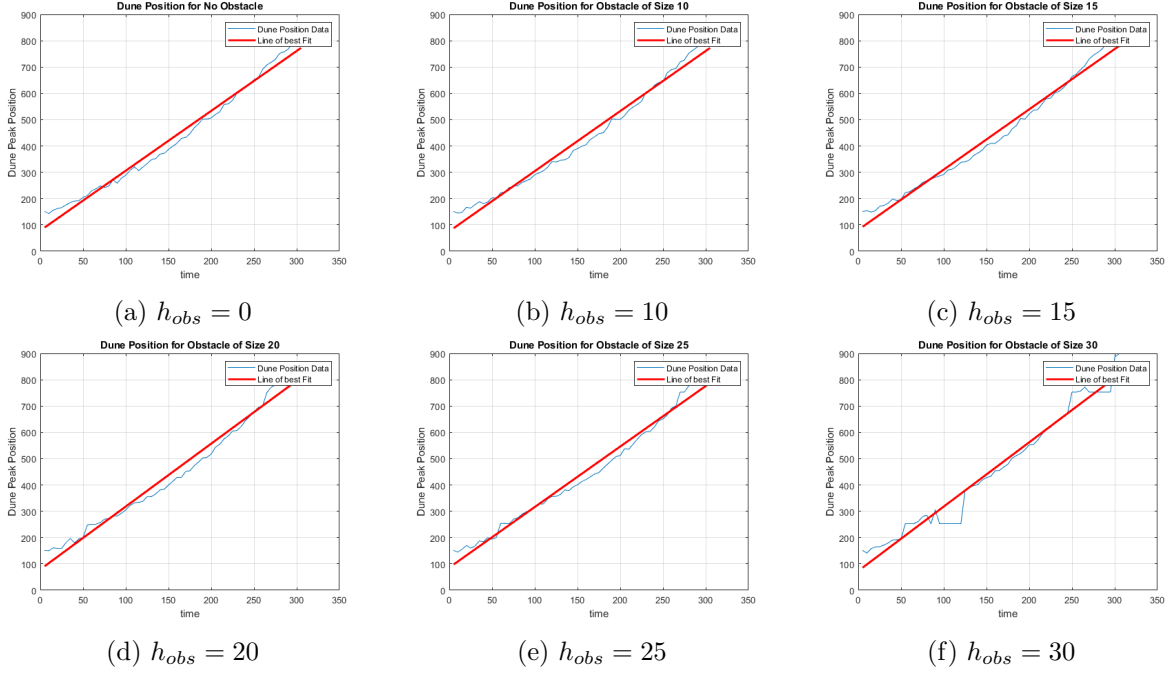
7

(a) $h_{obs} = 0$ (b) $h_{obs} = 10$ (c) $h_{obs} = 15$

(d) $h_{obs} = 20$ (e) $h_{obs} = 25$ (f) $h_{obs} = 30$

Figure 9: Dune position as a function of time for different obstacle sizes h_{obs}.

h_{obs}	$A(t=0)$	$A(t=100)$	$A(t=300)$	Average Dune Velocity
0	303.3	302.3	293.6	2.2745
10	303.3	285.3	285.6	2.2835
15	303.3	294.3	277.3	2.2923
20	303.3	276	266.6	2.2901
25	303.3	240.7	201.1	2.2993
30	303.3	179.3	132	2.4444

Table 1: Table of values for dune cross section areas (A) and velocities with respect to obstacle size h_{obs}. $t = 100$ corresponds to the time immediately after the first collision with the obstacle, and $t = 300$ corresponds to the time immediately after the second collision. All units are arbitrary.

observed a convincing interaction between sand dunes and obstacles, despite the simple model. Our findings may prove valuable in real life because the model we designed is only composed of simple mathematical formulas, which means that users can get results quickly after inputting parameters. At the same time, our model has high accuracy, which greatly improves the usability of our model. Common use scenarios such as helping designers determine the height of buildings in the desert to prevent sand accumulation. It can also help the government to predict the route of a large area of sand dunes in advance so as to achieve the goal of forestation on the route of dunes in advance as to prevent and control desertification. However, there are still some problems to be clarified in this model. First of all, no matter how high the obstacle in our model is, some sand particles will still fall on it, which is unusual in reality. Second, in this model, we assume that the sand plate remains intact during transportation, but the sand may scatter when it touches the ground. The true trajectory of sand particles needs further study. Third, our model is not universal because we assume that several extensions of our work are noteworthy. First of all, in order to make the model more applicable to reality, we hope to diversify the shape of obstacles and further study the impact of obstacles on the shape of sand dunes because the shape of objects in the real desert may be irregular. Secondly, we want to

8

explore how the physical properties of sand affect the dynamics of sand dunes. For example, how do sand dunes move in deserts with uneven humidity and different particle types? This study can help people better predict the movement of sand dunes. Thirdly, compared with only one obstacle in this model, the addition of multiple obstacles will greatly enhance the practicability of the model. Fourth, we want to know how erosion affects obstacles in the long term. More factors can be considered, such as the most vulnerable part of the barrier and the resistance of the barrier material. Finally, the wind direction in the model will become more complex, from the original wind mainly acting on the sand dunes from a single direction to multiple winds of different strengths acting on the sand dunes at the same time. This can also be closer to the desert scene in the real world.

5 Variables

TABLE 2 Simulation Parameters	
Parameter	Value
Lattice Size	500*500
Slab Aspect Ratio	1/3
Angle of repose	
to the nearest neighbor	$\tan^{-1}(2/3) = 33.7°$
to the Second nearest neighbor	$\tan^{-1}(2/3/\sqrt{2}) = 25.2°$
Shadow Zone Angle	15°
transport length at the reference height shear-velocity-increase:	$L_0 = 5 (unless specified in the text)$
linear coefficient	$C_1 = 0.4$
non-linear coefficient	$C_2 = 0.002$
erosion probability:	
outside shadow zone	Same at every site
in shadow zones	0.0
deposition probability:	
outside shadow zone:	$P_s = 0.6$
with at least a slab	$P_s = 0.6$
without a slab	$P_{ns} = 0.4$
in shadow zones	$P_s = P_{ns} = 1.0$
Obstacle Sizes	$h_0 = 10 \quad h_5 = 30$
	(increase it by 5 units at a time)

References

[1] Bruno Andreotti, Philippe Claudin, and Stéphane Douady. Selection of dune shapes and velocities. Part 1: Dynamics of sand, wind and barchans. *The European Physical Journal B*

- *Condensed Matter*, 28(3):321–339, August 2002. arXiv:cond-mat/0201103.

[2] Karol A. Bacik, Priscilla Canizares, Colm-cille P. Caulfield, Michael J. Williams, and Nathalie M. Vriend. Dynamics of migrating sand dunes interacting with obstacles. *Physical Review Fluids*, 6(10):104308, October 2021. Publisher: American Physical Society.

[3] Steven R. Bishop, Hiroshi Momiji, Ricardo Carretero-González, and Andrew Warren. Modelling desert dune fields based on discrete dynamics. *Discrete Dynamics in Nature and Society*, 7:275454, January 1900. Publisher: Hindawi Publishing Corporation.

[4] Hiroshi Momiji, Ricardo Carretero-González, Steven R Bishop, and Andrew Warren. Simulation of the effect of wind speedup in the formation of transverse dune fields. *Earth Surface Processes and Landforms*, 25(8):905–918, 2000. _eprint: https://onlinelibrary.wiley.com/doi/pdf/10.1002/1096-9837%28200008%2925%3A8%3C905%3A%3AAID-ESP112%3E3.0.CO%3B2-Z.

[5] Eric Parteli. Physics and Modeling of Wind-Blown Sand Landscapes. In *Reference Module in Earth Systems and Environmental Sciences*. January 2021. Journal Abbreviation: Reference Module in Earth Systems and Environmental Sciences.